

Analysis of Displacement Sensitive Twin Tube Shock Absorber

Mr.M.A.Jadhav¹, Prof. S.B. Belkar², Prof.R.R.Kharde³

¹K.J.Collge of Engineering & Management Research, Lecturer, Pune, ²Pravara Rural College of Engineering, Professor,Loni, ³Pravara Rural College of Engineering, Professor,Loni .

Abstract:- This paper includes the analysis of displacement sensitive twin tube shock absorber. The function of all the components like piston valve , compression and rebound chamber and the flow analysis of the fluid through these valves is studied in detail. Damping characteristics of automotive is analysed by considering the performance of displacement-sensitive shock absorber (DSSA) for the ride comfort. The proposed model of the DSSA is considered as two modes of damping force (i.e. soft and hard) according to the position of piston. For the simulation validation of vehicle-dynamic characteristics, the DSSA is mathematically modelled by considering the fluid flow in chamber and valve in accordance with the hard, transient and soft zone. And the vehicle dynamic characteristic of the DSSA is analysed using quarter car model.

Keywords:- Displacement sensitive twin tube shock absorber, vibration transmissibility, force transmissibility.

I. INTRODUCTION

The dampers employed in automotive suspension are mostly designed to yield asymmetric damping characteristics in compression and rebound in order to achieve a better compromise between ride, road-holding, handling and control performance of the vehicle. Owing to considerably higher wheel velocity in the upward direction, when compared to that in the downward direction, the dampers provide significantly higher damping force in rebound. The non-linear and asymmetric damping properties of shock absorbers have been widely characterized in terms of hysteresis and peak force-peak velocity characteristics. A number of analytical models based upon fluid flows through damper orifices and valves, and semi-empirical formulations have been developed to characterize the asymmetric force-velocity characteristics. Since these models require prior knowledge of various coefficients to be derived from the measured data for a specific damper, their applications have been limited for analysis of vehicle ride and handling.[1]

Shock absorber is an important part of automotive which has an effect on ride characteristics such as ride comfort and driving safety. There are several kinds of automotive shock dampers such as position-sensitive damping, acceleration-sensitive damping, and continuous damping control. Displacement-sensitive shock absorber (DSSA), which is also called stroke-dependent shock absorber, and has a similar structure compared with conventional passive shock absorber. Nevertheless, the DSSA has additional flow passages such as displacement-sensitive orifice at the cylinder wall. The DSSA has two modes of damping force according to piston stroke.[1]

When piston stroke is in the range of displacement-sensitive orifice, the leakage occurs through this orifice. In this range, the damping force become low compared with the passive shock absorber. On the other hand, when the piston stroke is out of range of displacement-sensitive orifice, leakage through the orifice is blocked. In this range, the damping force becomes high because of leakage block. Such a DSSA improves ride comfort on the paved road driving conditions because of low damping force caused by small piston stroke. Also, the driving safety is improved when the vehicle is driving on rough roads or bumper roads because of high damping force caused by large piston stroke and high-vibration amplitude. The DSSA can keep ride comfort and driving safety as well.[1]

There have been several studies about shock absorber. In the studies the transient characteristics of displacement-sensitive orifice were not considered and the performance of the vehicle with the DSSA was not verified. In general, those studies are insufficient to understand the dynamic characteristics of DSSA completely to judge the handling and ride comfort of automotive. Therefore, in this study a new mathematical and simulation model of the DSSA is proposed and analysed, which considered the transient range of displacement-sensitive orifice of the DSSA. And the vehicle dynamic characteristics of the proposed model are evaluated in the time and frequency domain using quarter car-simulation model. The results of the dynamic characteristics and the performance of the DSSA are compared with the passive shock absorber to prove the effectiveness. In

order to reduce the vibrations in the revolving machines and the mechanical systems, the dynamic absorbers are often used in various mechanical applications (Crankshaft, rotor of the wings of a helicopter, etc.). In the case of the real structures a linear model will be insufficient to describe the dynamic behaviour correctly. It thus appears natural to introduce non-linear models of structures which are able to predict the dynamic behaviour of the real structures. The solutions of these non-linear problems are obtained by approximate methods which exploit iterative algorithms. In the literature, several methods were proposed to approach the solution of the mechanical systems subjected to dynamic stresses.[1]

II. METHOD OF ANALYSIS OF SHOCK ABSORBER

A. Modelling of DSSA

Fig.1 illustrates the configuration of a typical twin-tube-type passive shock absorber of an automotive system. Basically the shock absorber consists of a piston, which moves up and down along fluid-filled cylinder. The cylinder is fastened to the axle or wheel suspension, and the piston is connected via the piston rod to the frame of the vehicle. As the piston is forced to move with respect to the cylinder, a pressure differential is developed across the piston causing the fluid to flow through orifices and valves in the piston. The portion of the cylinder above the piston is known as the rebound chamber, and the portion of the cylinder below the piston is known as the compression chamber, and the volume which surrounds the cylinder is known as the reservoir chamber. The reservoir chamber is partially filled with fluid and partially filled with a gas phase, normally air. The fluid flow between the compression and reservoir chambers passes through the body valve assembly at the bottom of the compression chamber.

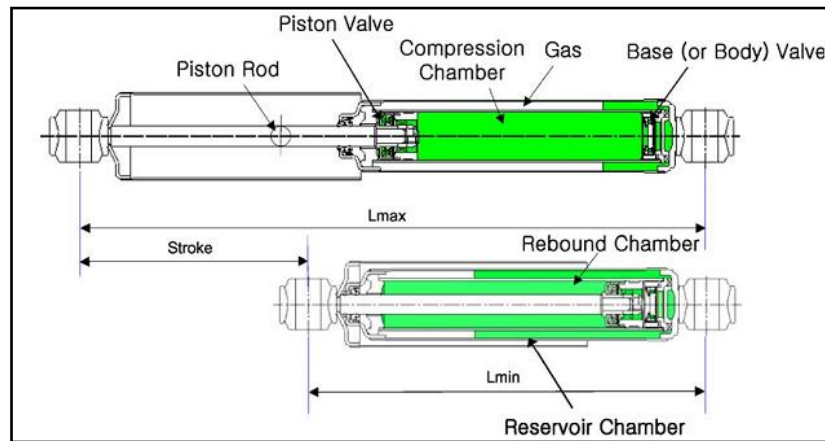


Fig.1 Schematic diagram of typical twin-tube-type passive shock absorber of an automotive system

Fig.2 shows the configurations of the piston valve assembly and the body valve assembly and their part of the shock absorber. As can be observed in Fig.2, the DSSA has an additional flow passage in the cylinder wall of a typical passive shock absorber. And these displacement-sensitive orifices can be divided into three zones such as the soft, transient and hard zone. Here, the transient zone has tapered scheme to avoid abrupt changes of damping force. Fig.3 illustrates the analytic model of the DSSA, which describes a fluid-flow pattern according to piston movement.

The fluid flows at the compression stroke can be divided into two flows such as Q_r and Q_c . The first Q_r is a flow which flows from the compression chamber to the rebound chamber through the piston valve (1) and the other Q_c is a flow which flows from the compression chamber to the reservoir chamber through body valve (2), where the valve numbers are noted in Fig.2. The flow Q_r , which flows through the piston valve, can be divided into three flows Q_{ri} , Q_{ro} and Q_{rd} . The flow Q_{ri} flows through the bleed valve (4). The flow Q_{ro} flows through intake valve (6) and the flow Q_{rd} flows through displacement-sensitive orifice (9) of piston valve, respectively. The flow Q_c , which flows through body valve (2) at the compression stroke, can be divided into two flows Q_{ci} and Q_{cf} . The flow Q_{ci} flows through the bleed valve and the flow Q_{cf} flows through a blow-off valve. On the contrary, at the rebound stroke the fluid flows can be divided into two flows Q_r^* and Q_c^* : The first Q_r^* is a flow which flows from the rebound chamber to the compression chamber through piston valve (1) and the other one Q_c^* is a flow which flows from the reservoir chamber to the compression chamber through body valve (2).

The flow Q_c^* ; which flows through body valve (2), can be divided into two flows Q_{ci} and Q_{co} . The flow Q_{ci} flows through the bleed valve and the flow Q_{co} flows through suction valve (7). Also, the flow Q_r^* ; which flows through piston valve (1), can be divided into three flows Q_{ri} , Q_{rf} and Q_{rd} . The flow Q_{ri} flows through bleed valve (4), the flow Q_{rf} flows through blow off valve (5) and the flow Q_{rd} flows through the displacement-sensitive orifice, respectively.

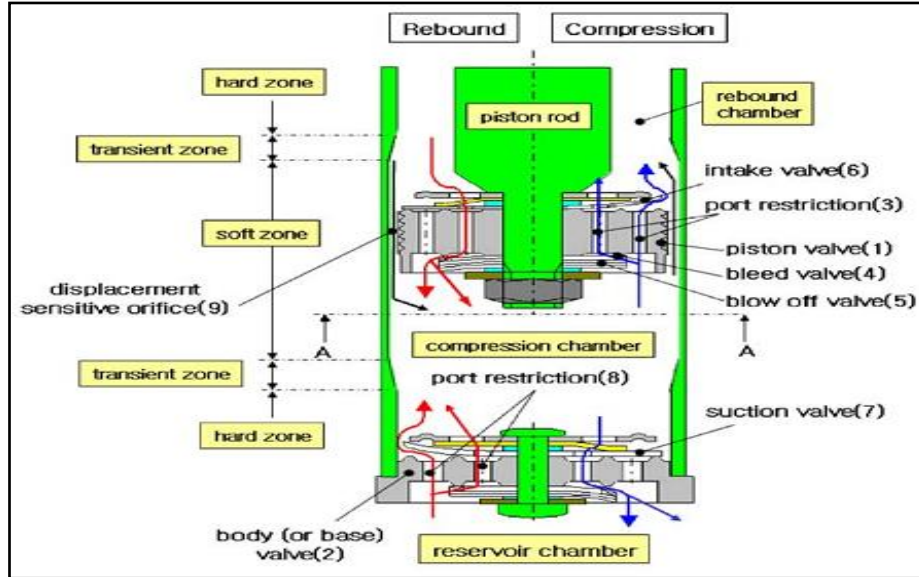


Fig.2 Fluid flow pattern of DSSA at compression and rebound stroke[1]

B. Flow continuity equations at the compression and rebound chamber

The flow continuity equation of the compression chamber at the rebound stroke, as described in Fig.3, can be expressed as follows:

$$-\frac{V_c}{K} \frac{\partial P_c}{\partial t} = -A_p \dot{x} + (Q_r^* + Q_c^*) \quad (1)$$

The flow continuity equation of the compression chamber at the compression stroke can be expressed as follows:

$$-\frac{V_c}{K} \frac{\partial P_c}{\partial t} = A_p \dot{x} - (Q_r + Q_c) \quad (2)$$

where K is a bulk modulus of elasticity of working fluid, V_c is a volume of compression chamber, P_c is a pressure of compression chamber, A_p is an area of piston and \dot{x} is a velocity of piston.

Similar way, the flow continuity equation of the rebound chamber at the rebound stroke can be expressed as follows:

$$-\frac{V_r}{K} \frac{\partial P_r}{\partial t} = (A_p - A_{rod}) \dot{x} - Q_r^* \quad (3)$$

Similar way, the flow continuity equation of the rebound chamber at the compression stroke can be expressed as follows:

$$-\frac{V_r}{K} \frac{\partial P_r}{\partial t} = (A_p - A_{rod}) \dot{x} + Q_r \quad (4)$$

Where V_r is a volume of rebound chamber, P_r is a pressure of rebound chamber and A_{rod} an area of piston rod.

C. Flow equations at the compression stroke and rebound stroke

The flow rate of the piston valve Q_r which flows between the rebound and compression chambers at the compression stroke can be expressed as follows:

$$Q_r = Q_{ri} + Q_{ro} + Q_{rd} \quad (5)$$

Here, each flow rates can be obtained as follows:

$$Q_{ri} = C_d A_{pb} \sqrt{\frac{2(P_c - P_{d1})}{\rho}} = C_d A_{d1} \sqrt{\frac{2(P_{d1} - P_r)}{\rho}} \quad (6)$$

$$Q_{ro} = C_d A_{d2} \sqrt{\frac{2(P_c - P_{d2})}{\rho}} = Q_{im} \frac{(P_{d2} - P_{icr})}{(P_{im} - P_{icr})} \quad (7)$$

Here, when $P_{d2} < P_{icr}$, Q_{ro} becomes zero.

$$Q_{rd} = C_d A_{ds}(x) \sqrt{\frac{2(P_c - P_r)}{\rho}} \quad (8)$$

$$A_{ds}(x) = \begin{cases} w \left\{ \frac{h}{z_2} (x + z_1) + h \right\} & (z_1 < x \leq (z_1 + z_2)) \\ wh & (-z_1 < x \leq z_1) \\ w \left\{ -\frac{h}{z_2} (x - z_1) + h \right\} & (-(z_1 + z_2) < x \leq -z_1) \end{cases}, \quad (9)$$

where C_d is a coefficient of discharge and A_{pb} is a bleed valve (4) orifice area of piston valve (1).

A_{d1} and A_{d2} are areas of piston valve (1) port restriction (3), P_{d1} and P_{d2} are pressures at piston valve (1) port restriction (3), Q_{im} is a maximum flow rate of the intake valve (6), P_{icr} is a cracking pressure of intake valve (6), P_{im} is a pressure of intake valve (6) at the maximum flow rate Q_{im} and A_{ds} is an area of the displacement-sensitive orifice.

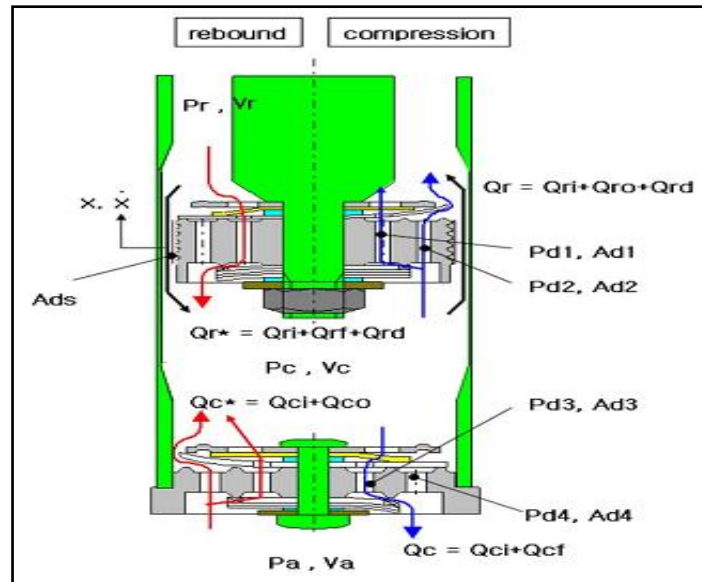


Fig.3 Schematic diagram of fluid flow and pressure at compression and rebound stroke.[1]

The flow rate Q_{rd} becomes zero when the displacement of the piston detaches from displacement-sensitive orifice, and the flow rate of the body valve Q_c , which flows between the reservoir and compression chambers. At the compression, stroke can be expressed as follows:

$$Q_c = C_d A_{a3} \sqrt{\frac{2(P_c - P_{a3})}{\rho}} = Q_{ci} + Q_{cf} \quad (10)$$

Each flow rates of Eq. (10) can be obtained as follows:

$$Q_{ci} = C_d A_{bb} \sqrt{\frac{2(P_{a3} - P_a)}{\rho}} \quad (11)$$

$$Q_{cf} = Q_{bm} \frac{(P_{a3} - P_{bcr})}{(P_{bm} - P_{bcr})} \quad (12)$$

Here, when $P_{a3} < P_{bcr}$; Q_{cf} becomes zero. A_{bb} is a bleed valve orifice area of body valve (2), A_{d3} is a port restriction area (8) of body valve (2), P_a is a pressure of reservoir chamber, Q_{bm} is a maximum flow rate of the blow-off valve at the body valve, P_{bcr} is a cracking

pressure of the blow-off valve at the body valve and P_{bm} is a pressure of the blow-off valve at the maximum flow rate at the body valve.

The flow rate of the piston valve Q_r^* which flows between rebound and compression chambers at the rebound stroke can be expressed as follows:

$$Q_r^* = Q_{ri} + Q_{rf} + Q_{rd} \quad (13)$$

$$Q_{ri} = C_d A_{pb} \sqrt{\frac{2(P_{d1} - P_c)}{\rho}} \quad (14)$$

$$Q_{rf} = Q_{pm} \frac{(P_{d1} - P_{pcr})}{(P_{pm} - P_{pcr})} \quad (15)$$

Here when $P_{d1} < P_{pcr}$, Q_{rf} becomes zero.

$$Q_{rd} = C_d A_{ds}(x) \sqrt{\frac{2(P_r - P_{cr})}{\rho}} \quad (16)$$

Where Q_{pm} is a maximum flow rate of blow-off valve (5) at the piston valve, P_{pcr} is a cracking pressure of the blow-off valve at the piston valve and P_{pm} is a pressure of the blow-off valve at the maximum flow rate of the piston valve. Q_{rd} becomes zero when the displacement of the piston detaches from the displacement-sensitive zone. And the flow rate of body valve Q_c^* which flows between the reservoir and compression chambers at the rebound stroke can be expressed as follows:

$$Q_c^* = Q_{ci} + Q_{co} \quad (17)$$

$$Q_{ci} = C_d A_{bb} \sqrt{\frac{2(P_{a3} - P_a)}{\rho}} = C_d A_{d3} \sqrt{\frac{2(P_{d3} - P_c)}{\rho}} \quad (18)$$

$$Q_{co} = C_d A_{d4} \sqrt{\frac{2(P_a - P_{d4})}{\rho}} = Q_{sm} \frac{(P_{d4} - P_{scr})}{(P_{sm} - P_{scr})} \quad (19)$$

Here, when $P_{d4} < P_{scr}$; Q_{co} becomes zero, where A_{d4} is a port restriction (8) area of the body valve. P_{d4} is a pressure at the body valve port restriction (8), Q_{sm} is a maximum flow rate of suction valve (7). P_{scr} is a cracking pressure of the suction valve and P_{sm} a pressure at the maximum flow rate of the suction valve.[1]

D. Flow analysis at the reservoir chamber

Because the piston rod passes through the rebound chamber, and is connected to the rebound of the piston, the area of the rebound side is less than the area of the compression side of the piston. Accordingly, as the piston moves, the combined volume of the compression and rebound chambers changes by an amount equivalent to the inserted, or withdrawn piston rod volume. The amount of fluid equivalent to the inserted, or withdrawn piston rod volume must be transferred to, or from, the reservoir chamber which normally surrounds the cylinder. Air pressure of the reservoir chamber can be expressed as an ideal gas equation as follows:

$$P_a V_a = m_a RT \quad (20)$$

Where P_a is an air pressure of the reservoir chamber, V_a is an air volume of reservoir chamber, m_a is an air mass of reservoir chamber, R is a gas constant and T is the temperature of air in the reservoir chamber. Generally, the mass of air is assumed constant because the chamber is sealed, and the temperature T of the reservoir chamber is assumed constant to simplify the analysis. Accordingly, the air of the reservoir chamber can be expressed as an ideal gas equation as follows:

$$P_a V_a = \text{constant} \quad (21)$$

$$V_a(t) = V_{a0} - \int Q_c dt \quad (22)$$

Where V_{a0} is an initial air volume of reservoir chamber. Therefore the air pressure variation of the reservoir chamber can be obtained from Eqs.(20)and (22)as follows

$$P_a = \frac{m_a RT}{V_{a0} \int Q_c dt} \quad (23)$$

E. Damping force of shock absorber

The damping force of shock absorber is determined by the forces acting on the both sides of the piston. And the friction forces are another factor that determines damping force. Nevertheless, in this study, the friction forces are ignored to simplify the analysis. Fig.4 shows free body diagram of the piston considering the damping force.[1]

By considering the forces acting on the piston, the damping force can be obtained as follows:

$$F_{damping} = P_r A_r - P_c A_c \pm F_{friction} \quad (24)$$

$$A_r = A_p - A_{rod} \quad (25)$$

Where $F_{damping}$ is a damping force. $F_{friction}$ is the friction force acting on the piston rod.

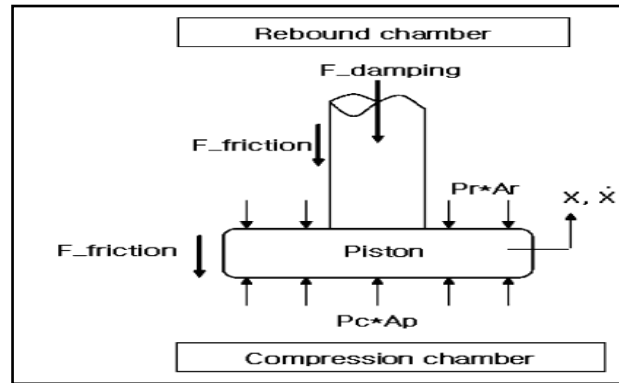


Fig.4. Free body diagram of the piston.[1]

F. DYNAMIC EQUATIONS OF THE SYSTEM

A cutaway view of the longitudinal section of the twin tube hydraulic shock absorber is shown in Fig.5, in which the internal tube is partitioned into A and B chambers by the piston. Whenever the piston is forced to move down during a compressive shock, the oil in Chamber B is compressed to flow to Chamber A and Chamber C through some valves and orifices, as seen the above arrows in Fig.5. Whenever the piston is forced to move up during a tensile shock, the oil in Chamber A and Chamber C flows to Chamber B through the other valves and orifices, as shown the below arrows in Fig. 4.1. The piston has several orifices, all closed at one end by a metallic plate, spring-loaded to the piston by two springs consisting of two folds washers. The valve does not open until the difference in pressure acting on both piston sides overcomes the force of the preloaded valve springs. When the pressure relief (or ‘‘blow-off’’) valve opens, the characteristics of the valve springs control the amount of valve opening, which conduct is approximately piecewise linear.

For the nonlinear analysis of the hydraulic shock absorber, a dynamic model of the suspension vibration quarter car system of three degrees of freedom under a sine excitation on the absorber base joint is proposed, as shown in Fig.6. The harmonic motion is transferred directly to the absorber tube and suspension spring by the rubber bush through the base joint. The piston damping force works on the body by the upper and lower rubber washers.[9]

Therefore, the kinematic energy T of the dynamic system can be expressed in terms of generalized coordinates as

$$T = \frac{1}{2} m_1 \dot{x}_1^2 + \frac{1}{2} m_2 \dot{x}_2^2 + \frac{1}{2} m_3 \dot{x}_3^2 \quad (1)$$

in which m_3 is the total mass of the upper and lower rubber washers, piston and piston rod, m_1 is the total mass of half suspension spring and the body, and m_2 is the total mass of half suspension spring, spring tray, rubber bush and tube. The potential energy E of the system may be presented also in terms of generalized coordinates as

$$E = \frac{1}{2} k_u (x_3 - x_1)^2 + \frac{1}{2} k_l (x_2 - x_1)^2 + \frac{1}{2} k_d (x_2 - x_0)^2 \quad (2)$$

in which k , k_u , k_l and k_d are, respectively, stiffness coefficients of the suspension coil spring, upper and lower rubber washers, and rubber bush. The dissipative energy D of the system can be given in terms of generalized coordinates as

$$D = \frac{1}{2} c_u (\dot{x}_3 - \dot{x}_1)^2 + \frac{1}{2} c_l (\dot{x}_3 - \dot{x}_1)^2 + \frac{1}{2} c (\dot{x}_3 - \dot{x}_1)^2 + \frac{1}{2} c_d (\dot{x}_2 - \dot{x}_0)^2 \quad (3)$$

where c , c_u , c_l and c_d are, respectively, damping coefficients of the absorber piston-tube interface, upper and lower rubber washers and rubber bush, x_0 sine displacement, A and x amplitude and frequency of the input, x_1 , x_2 , and x_3 generalized coordinates of the dynamic system.

Accordingly, the Lagrangian equations governing the motion of the 3-DOF vibration system may be expressed of the following form as

$$\frac{d}{dt} \left(\frac{\partial T}{\partial \dot{x}_j} \right) - \frac{\partial T}{\partial x_j} + \frac{\partial E}{\partial x_j} = - \frac{\partial D}{\partial \dot{x}_j} + Q \quad (4)$$

where x_j is the j th generalized coordinate of the system ($j = 1, 2$ and 3) and Q is the generalized force corresponding to external excitation.

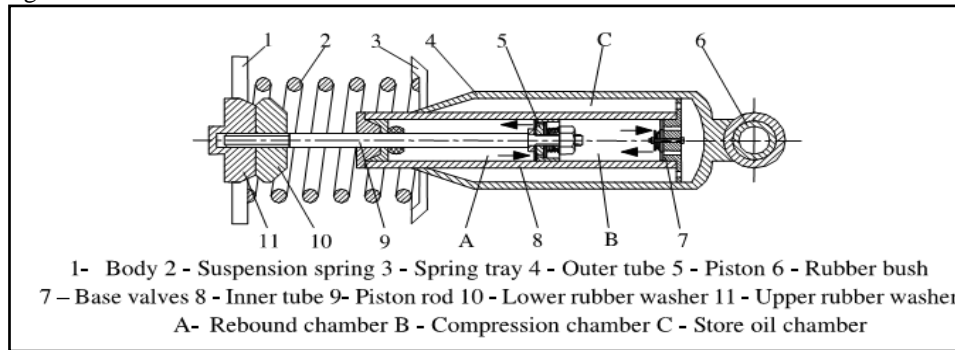


Fig.5. A cutaway view of the twin tube shock absorber.[9]

By setting $X = (x_1, x_2, x_3)^T$ and $Q = [x_0]$, insertion of Eqs. (1)–(3) into Eq. (4) results in the equation of motion in matrix form as

$$[M] \ddot{X} + [K]X + [C] \dot{X} = [K_d]Q + [C_d] \dot{Q} \quad (5)$$

Where

$$[M] = \begin{bmatrix} m_1 & 0 & 0 \\ 0 & m_2 & 0 \\ 0 & 0 & m_3 \end{bmatrix},$$

$$[K] = \begin{bmatrix} -(k + k_u + k_1) & k & (k_u + k_1) \\ k & -(k + k_d) & 0 \\ (k_u + k_1) & 0 & -(k_u + k_1) \end{bmatrix}$$

$$[C] = \begin{bmatrix} -(c_u + c_1) & 0 & (c_u + c_1) \\ 0 & (c + c_d) & c \\ (c_u + c_1) & c & -(c + c_u + c_1) \end{bmatrix}$$

and the stiffness and damping matrices corresponding to the excitation are as follows:

$$[K_d] = [0, -k_d, 0]^T$$

$$[C_d] = [0, -c_d, 0]^T$$

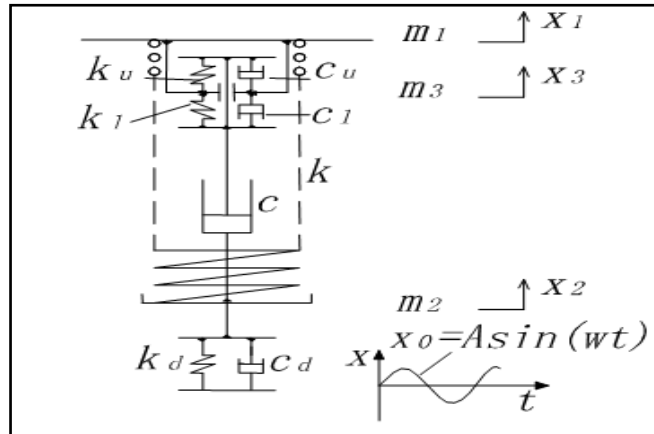


Fig.6 The dynamic model for the absorber.[9]

Stiffness and damping properties of the absorber system are nonlinear in the practical (Blundell, 1998). For the purpose of reducing laborious efforts in nonlinear analysis of the system model, some simplifications should be imposed to the mathematic model in Eq. (5). The suspension spring stiffness is usually linear, and according to real testing results, stiffnesses and damping coefficients of the rubber components may be treated approximately as linearized. Thus, k , k_u , k_1 , k_d , c_u , c_1 and c_d are reduced to be constants, except that the damping coefficient c remains nonlinear.[9]

G. EXPERIMENTAL PROCEDURE

a. Experimental setup

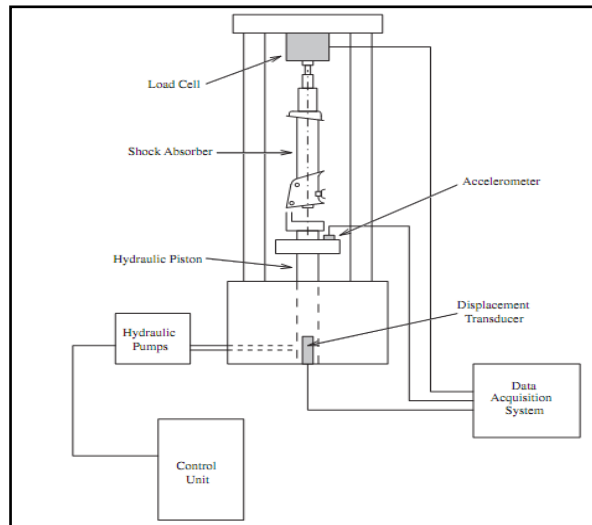


Fig. 7. Schematic diagram of the shock absorber test bench

b. Procedure

Displacement sensitive shock absorber is actuated with the help of hydraulic actuator .The apparatus and experimental strategy are shown in Fig.7. Briefly, data will be recorded from and absorber that was constrained to move in only one direction in order to justify the assumption of single degree-of-freedom (SDOF) behavior. The top of the absorber was fixed to a load cell so that the internal force could be measured directly (it was found that inertial forces were negligible).

As previous experimental evidence had suggested that the dampers were strongly nonlinear and also frequency dependent, it was decided to carry out the first set of tests at constant frequency in order to isolate the effects of the nonlinearity. However, if the displacement response of a system is a single harmonic, force data are only available above the corresponding phase trajectory that is simply an ellipse. For this reason periodic signals are of little use for generating restoring force surfaces; ideally, force data are required that are evenly distributed in the phase plane. In order to meet this requirement without violating the requirement of a single response frequency, several tests were carried out at each frequency, each subtest was for a different response amplitude. Once the subtest data were assembled at each frequency, this procedure gave force data over a set of concentric curves in the phase plane. This allowed the construction of a force surface for each test frequency, an

isofrequency surface. Comparison of such surfaces then indicates if the absorber under test was frequency dependent.

Because automotive dampers or shock absorbers are designed to be significantly nonlinear, it is untenable to model them as linear systems. In order to correctly simulate the behavior of such shock absorbers, it is essential that one characterizes the actual nonlinearities present in the structure. A traditional approach to characterization of the nonlinearities present in the shock absorber is accomplished by obtaining a force–velocity or characteristic diagram. The force data from a test are simply plotted against the corresponding velocity values. These diagrams show ‘hysteresis’ loops, that is, a finite area is enclosed within the curves. This hysteresis is a consequence of the position dependence of the force. Similar plots of force against displacement—work diagrams—can also be produced that convey information about the position dependence of the absorber. Fig.7 displays the characteristic diagram for a typical automotive shock absorber. These visualizations are not accurate enough to capture the dynamics of the system. The more comprehensive approach illustrated here is to use measured data to construct the restoring force surface for the absorber. This simultaneously displays the position and velocity dependence of the restoring force in the absorber without a priori knowledge of the structure.

The shock absorber test facility essentially took the same form as Fig.8. Facilities will be provided to add a parallel stiffness in the form of a spring of known characteristics and to load the system with an additional mass. This option was not used for the particular test described below. As the shock absorber is essentially an SDOF system under vertical excitation in this configuration. The excitation for the system was provided by the random signal generator of a spectrum analyzer, amplified and filtered into the interval 2–30Hz. The band-limited signal facilitates post-processing of measured data, for example, numerical differentiation or integration. The piezoelectric load cell provided a measurement of $x(t)$. The other signal measured was displacement, the required velocity and acceleration being arrived at by numerical differentiation. This decision was made because the actuator actually incorporates an LVDT displacement transducer that produces a high quality signal.

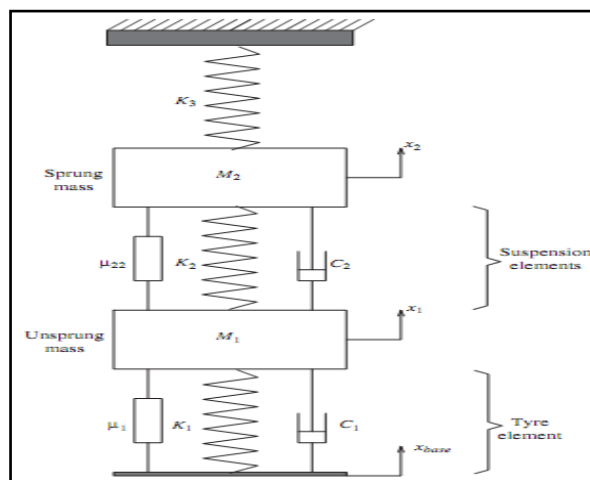


Fig.8 The suspension model for shock absorber.

c. Experimental damping characteristic of the absorber

In the analysis of dynamic responses, damping force–velocity curves which are characterized to be piecewise linearized, as shown in Fig.9, is applied to model the experimental damping characteristic of the average sense. Though the theoretical damping characteristic composed of three folded lines is distinguished from the experimental one, the piecewise linearized curves are preferably used in the computer simulation of the absorber dynamic behaviors during a working period. In fact, the absorber damping force F is a strongly nonlinear function of piston velocity V , and the behavior is not symmetrical versus velocity sign (compression and rebound). Moreover, different values of damping force can be obtained with the same value of piston velocity showed unsymmetrical hysteretic phenomenon in experiment on the MTS testing machine, as shown in Fig. 9. Using the internal fluid dynamic phenomenon with respect to a hydraulic shock absorber, the importance of different factors for the hysteretic phenomenon, such as oil compressibility, frequency dependent behavior and oil inertia was presented (Audenino and Belingardi, 1995). Oil compressibility causes elastic energy to be stored in the absorber. By increasing the oil compressibility, the area of the hysteretic loop also increases, reflecting a higher level of energy accumulation. The effect of excitation frequency is similar to the oil compressibility. When the excitation frequency is above 5 Hz, the hysteretic loop of the damping force–velocity is apparent in experiment. The oil inertia could also cause hysteretic loop with an area that increases as the

inductive effect increases, but maximum force remains the same regardless of the amount inertial effect. Other factors, for example the flow of hydraulic oil past sharp-edge orifices, restrictive passages and blow-off valves, as well as losses in joints, Coulomb friction, are involved in the analysis for the hysteretic damping force by some researchers (Audenino and Belingardi, 1995).

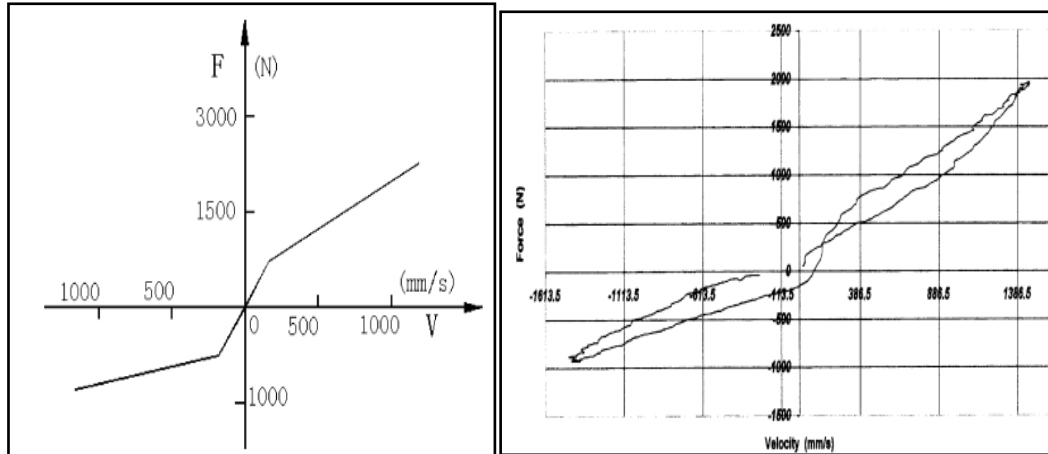


Fig. 9.(A) Piecewise linear damping force–velocity curve of the absorber. (B) Testing results for the hysteretic loop of the absorber

Fig. 10(a) shows the analysis result of suspension deflection of the displacement-sensitive mode using the DSSA in the time domain. Fig. 10(b) shows the analysis results of suspension deflection in the PSD for the four damping modes in the frequency domain. As shown in Fig.10, the response characteristic of the DSSA seems similar to the ones of passive shock absorber around the resonance frequency range of sprung mass. However, at the resonance frequency of un-sprung mass, the DSSA shows soft damping characteristics.

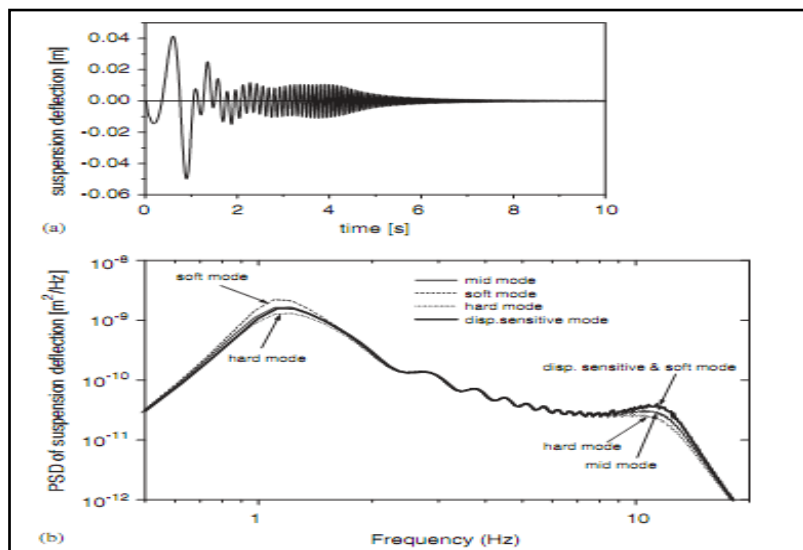


Fig. 10. Suspension deflection of displacement-sensitive mode: (a) time response of suspension acceleration and (b)PSD of suspension deflection

III. CONCLUSIONS

In this study ,a new mathematical dynamic model of the DSSA is proposed. The fluid rate and the damping force of a shock absorber of an automotive system was theoretically formulated. The analysis results of the proposed mathematical dynamic model of the DSS showed similar results of the corresponding experimental study. It is shown that the damping force could be efficiently calculated according to the excitation. And the vehicle dynamic characteristic of the DSSA is analysed using quarter car model. Several damping properties of the automotive shock absorber that are of interest in vehicle vibration applications are reviewed in accordance with the ride comfort problem. The simulation results of frequency response are compared with the ones on passive shock absorber. From the analysis results of the DSSA, the ride comfort of the DSSA increased. The

results reported herein will provide a better understanding of the shock absorber. Moreover, it is believed that those properties of the results can be utilised in the dynamic design of the automotive system.

ACKNOWLEDGMENT

And finally this day has come. I am presenting the paper with great pride. There are too much efforts of gardener to yield the beautiful flowers. So we should not forget him while praising flower. It is a matter of gratification for me to pay my respects and acknowledgements to all those who have imparted knowledge and helped me to complete my report.

I would first like to acknowledge the great contribution and support I have received in this endeavor from Guide Prof.S.B.Belkar . His in depth guidance and inspiration for me will be of great help to tackle any kind of problems likely to be met in the future.

I expressed my sincere thanks to Head of Dept. Prof. R.R. Kharde for their valuable guidance. I much obliged towards all the staff members, librarians, and my friends those supported directly and indirectly. I will keep my improvement curve on the rise and thereby enhance the reputation of my College.

REFERENCES

- [1]. Choon-Tae Leea, Byung-Young Moon,2006, "Simulation and experimental validation of vehicle dynamic characteristics for displacement-sensitive shock absorber using fluid-flow modeling" Department of Mechanical and Intelligent Systems Engineering, Busan National University, 30 Changjeon-dong, Keumjeong-ku, Busan 609-735, Republic of Korea.
- [2]. Sahin Yildirim, Ibrahim Uzmay,2003, "Neural network applications to vehicle's vibration analysis", Machine Dynamics and Theory Research Laboratory, Engineering Faculty, Department of Mechanical Engineering, Erciyes University, 38039 Kayseri, Turkey.
- [3]. M.-L. Bouazizi, S. Ghanmi,2009, "Robust optimization of the non-linear behaviour of a vibrating system", Nabeul Preparatory Engineering Institute (IPEIN), University of 7 Novembre, 8000 M'rezgua, Nabeul, Tunisia.
- [4]. Keith Wordena, DarylHickey,2009, "Nonlinear system identification of automotive dampers: A time and frequency-domain analysis", Dynamics Research Group, Department of Mechanical Engineering, University of Sheffield, Mappin Street, Sheffield S1 3JD, UK
- [5]. A.K. Samantaray,2009, "Modeling and analysis of preloaded liquid spring/damper shock absorbers", Department of Mechanical Engineering, Indian Institute of Technology, 721302 Kharagpur, India
- [6]. Yang Pinga, Tan Yonghongb,,2006, "Measurement, simulation on dynamic characteristics of a wire gauze–fluid damping shock absorber" Research Center of Micro-Nano Science and Technology, School of Mechanical Engineering, JiangSu University, Zhenjiang 212013, PR China
- [7]. Maciejewskia, L.Meyer,2009, "Modelling and multi-criteria optimisation of passive seat suspension vibro-isolating properties", Koszalin University of Technology, Department of Mechatronics and Applied Mechanics, Raclawicka 15-17, Koszalin 75-256, Poland
- [8]. C. Rajalingham, S. Rakheja,2003, "Influence of suspension damper asymmetry on vehicle vibration response to ground excitation", Concave Research Center, Department of Mechanical Engineering, Concordia University, Montreal, Que., Canada H3G 1M8.
- [9]. Yanqing Liu, Jianwu Zhang,2002, "Nonlinear dynamic responses of twin-tube hydraulic shock absorber", School of Mechanical Engineering, Institute for Automotive Engineering, Shanghai Jiaotong University, 1954 Huashan Road, Shanghai 200030, China
- [10]. Y. Ping,2003, "Experimental and mathematical evaluation of dynamic behavior of an oil air coupling shock absorber", Department of Electronic Machinery, Guilin Institute of Electronic Technology, Guilin 541004, People's Republic of China
- [11]. N.F. du Plooy,2005, "The development of a tunable vibration absorbing isolator", Dynamic Systems Group, Department of Mechanical and Aeronautical Engineering, University of Pretoria, Pretoria 0002, South Africa.
- [12]. Jamil M. Renno , Brian R. Mace,2012, "Vibration modelling of helical springs with non-uniform ends" Institute of Sound and Vibration Research, University of Southampton, Southampton SO17 1BJ, United Kingdom
- [13]. W. Schiehlen ,B.Hu,2003, "Spectral simulation and shock absorber identification" Institute B of Mechanics, University of Stuttgart, Pfa enwaldring 9, D-70550 Stuttgart, Germany
- [14]. Walid Belgacem, Alain Berry, Patrice Masson, "Active vibration control on a quarter-car for cancellation of road noise disturbance", G.A.U.S., Mechanical Engineering Department, Universite ´ de Sherbrooke, Sherbrooke, QC, Canada J1K 2R1.s